Neurobiology of Aging 36 (2015) 1780–1791

Contents lists available at ScienceDirect

Neurobiology of Aging

journal homepage: www.elsevier.com/locate/neuaging

Neurotoxicity and synaptic plasticity impairment of N-acetylglucosamine polymers: implications for Alzheimer's disease

Ermanna Turano [a], Giuseppe Busetto [b,c], Silvia Marconi [a], Flavia Guzzo [d], Alessia Farinazzo [a], Mauro Commisso [d], Edoardo Bistaffa [a], Stefano Angiari [e], Salvatore Musumeci [f], Stefano Sotgiu [g], Bruno Bonetti [a,*]

[a] Section of Neurology, Department of Neurological and Movement Sciences, University of Verona, Verona, Italy
[b] Section of Physiology and Psychology, Department of Neurological and Movement Sciences, University of Verona, Verona, Italy
[c] Italian Institute of Neuroscience, Verona, Italy
[d] Department of Biotechnology, University of Verona, Verona, Italy
[e] Department of Pathology, University of Verona, Verona, Italy
[f] Department of Biomolecular Chemistry, National Research Council, Catania, Italy
[g] Department of Clinical and Experimental Medicine, University of Sassari, Sassari, Italy

ARTICLE INFO

Article history:
Received 16 June 2014
Received in revised form 18 December 2014
Accepted 26 December 2014
Available online 6 January 2015

Keywords:
Alzheimer's disease
N-acetylglucosamine
Amyloid
Neurotoxicity
LTP

ABSTRACT

We assessed whether polymers of *N*-acetylglucosamine (GlcNAc) have any pathogenetic role in Alzheimer's disease (AD). First, by using specific dyes, we found deposits of polymers of GlcNAc in sporadic but not in familial AD. We found that neurons and microglia exposed to GlcNAc and uridine diphosphate (UDP)-GlcNAc are able to form GlcNAc polymers, which display a significant neurotoxicity in vitro. Moreover, the exposure of organotypic hippocampal cultures to the same compounds led to synaptic impairment with decreased levels of syntaxin and synaptophysin. In addition, acute hippocampal slices treated with GlcNAc/UDP-GlcNAc showed a clear reduction of long-term potentiation of excitatory synapses. Finally, we demonstrated that microglial cells are able to phagocytose chitin particles and, when exposed to GlcNAc/UDP-GlcNAc, show cellular activation and intracellular deposition of GlcNAc polymers that are eventually released in the extracellular space. Taken together, our results indicate that both microglia and neurons produce GlcNAc polymers, which trigger neurotoxicity both directly and through microglia activation. GlcNAc polymer-driven neurotoxicity offers novel pathogenic insights in sporadic AD and new therapeutic options.

1. Introduction

The neuropathologic hallmarks of Alzheimer's disease (AD) are amyloid plaques and neurofibrillary tangles, with consequent synaptic impairment and neuronal loss (Querfurth and La Ferla, 2010). According to the so-called "amyloid cascade hypothesis," an imbalance between production and clearance causes the accumulation of insoluble amyloid-β (Aβ) protein (Abbott, 2008; Haas and Selkoe, 2007; Koffie et al., 2011; Querfurth and La Ferla, 2010; Selkoe, 2008; Turner et al., 2003). This hypothesis is mainly based on the studies of familial AD (FAD) and confirmed in the transgenic mice (Chapman et al., 1999; Games et al., 1995; Hsiao et al., 1996; Ittner et al., 2010; Lewis et al., 2001; Oakley et al., 2006; Oddo et al., 2003). This theory has led to human trials with different agents that could potentially decrease deposition or enhance the clearance of cerebral Aβ. Because of the poor results of these trials (Holmes et al., 2008; Lemere and Masliah, 2010), researchers have shifted their efforts from the Aβ dogma into other possible pathologic processes.

In this regard, an additional process that may contribute to AD pathogenesis is related to impaired brain glucose metabolism. A large body of evidence suggests a causal relationship between impaired brain glucose metabolism and neuronal damage in AD. In fact, cerebral glucose alteration precedes the appearance of clinical symptoms (Arvanitakis et al., 2004; Brownlee, 2001; Drzezga et al., 2003), and temporal hypoperfusion with decreased oxygen metabolism has been shown in AD (Ishii et al., 1996, 1998; Minoshima et al., 1995; Piert et al., 1996). In addition, decreased concentrations of glucose transporters type 1 and 3 have been found in the

* Corresponding author at: Section of Neurology, Department of Neurological and Movement Sciences, University of Verona, Ospedale Policlinico GB Rossi, P. Scuro 10, Verona 37134, Italy. Tel.: +39 0458124694; fax: +39 0458027492.
E-mail address: bruno.bonetti@univr.it (B. Bonetti).

0197-4580/$ – see front matter © 2015 Elsevier Inc. All rights reserved.
http://dx.doi.org/10.1016/j.neurobiolaging.2014.12.033

cerebral cortex of AD patients (Simpson and Davies, 1994; Simpson et al., 1994; Shah et al., 2012). The consequences at the neuronal level of such impaired glucose metabolism and the molecular mechanisms leading to neuronal damage are a matter of speculation. It is known that a dysregulation of glucose metabolism activates the hexosamine pathway (which usually accounts for about 5% of glucose metabolism), whose end product is *N*-acetylglucosamine (GlcNAc) (Brownlee, 2001; Love and Hanover, 2005; Shah et al., 2012).

In relation to these evidences, it is important to remember that amyloid plaques contain, beside Aβ, other molecules (O'Callaghan et al., 2008; Timmer et al., 2010; Van Horssen et al., 2003). Among them, we and others have found chitin-like deposits by Calcofluor staining in sporadic AD (Castellani et al., 2005; Sotgiu et al., 2008). Chitin is a linear β 1,4–linked polymer of GlcNAc and is the main component of the fungal cell walls and of the exoskeleton of arthropods (Glaser and Brown, 1957). Noteworthy, mammals lack chitin synthase, although hyaluronan synthase-1 (HAS-1) has been shown to convert uridine diphosphate (UDP)-GlcNAc to chito-oligosaccharides in vitro (Semino et al., 1996; Yoshida et al., 2002). However, neither the biosynthetic pathway of GlcNAc polymers in AD nor its possible contribution to the pathogenesis of the disease is known.

Therefore, to test whether GlcNAc polymers contribute to sporadic AD pathogenesis, we studied the effect of excess GlcNAc and UDP-GlcNAc in neuronal and microglial cell cultures and in organotypic brain cultures and acute brain slices, in terms of cytotoxicity, synaptic function, and cell activation.

2. Materials and methods

2.1. Patients

Paraffin-embedded central nervous system slides were obtained at autopsy from 13 sporadic human AD patients (age, 74.9 ± 11.1 years), 4 Down syndrome cases (age, 58.7 ± 4.8), 2 familiar AD with mutation on presenilin 1 (type: E280G and DELTA4) and 2 with mutation for APP717 (type: VAL-ILE), 4 cases of frontotemporal degeneration with dementia (age, 74.7 ± 6.7 years), and 9 age-matched nondemented controls (age, 77.2 ± 8.7 years) (MRC London Brain Bank for Neurodegenerative disease).

2.2. Cell lines and primary cultures

Murine N9 microglial cells and SH-SY5Y human neuroblastoma cells were cultured in RPMI media supplemented with 10% fetal bovine serum (FBS) (Euroclone, Milano, Italy); human fibroblasts were grown in 10% Dulbecco-Modified Eagle Medium (DMEM; Euroclone) with FBS. All cell lines were supplemented with 100-U/mL penicillin/streptomycin (P/S; Euroclone). Three days before and during any experiment, cells were incubated with 1% FBS in the previously mentioned culture medium. For immunocytochemical experiments, cells were seeded onto glass coverslips. Newborn BALB/c mice were used for the preparation of primary cultures. All animals (Harlan Laboratories Inc, S. Pietro di Natisone, Italy) were housed in pathogen-free conditions and treated according to the guidelines of Animal Ethical Committee of the University of Study of Verona. Primary microglial cultures were prepared from embryonic day (E)16 to E18 pups. Briefly, whole brains were removed and carefully cleared from the meninges. Cortices were subsequently minced into small pieces and treated with trypsin and DNase I (Sigma-Aldrich, St Louis, MO, USA) and centrifuged at 1000 rpm for 10 minutes. After digestion, pellets were resuspended in DMEM, 10% FBS, 100-U/mL P/S, and 2-mM glutamine. At 7–8 days, adherent cells were confluent and consisted of astrocytes and microglia. Microglial cells were removed by mild shaking from the astroglial layer. The non-adhering cells were centrifuged at 1000 rpm for 10 minutes and plated on uncoated plastic wells in DMEM with 10% FBS. Primary hippocampal neuronal cultures were prepared from E16 to E18 pups. The hippocampi were isolated and processed as described for microglia and plated on glass coverslips in 24 wells in neurobasal media, 10% FBS, 2-mM glutamine, P/S, and with B27 (Euroclone).

2.3. Preparation of chitin particles and induction of GlcNAc polymers

Chitin fragments were obtained as previously described (Shibata et al., 1997). Briefly, chitin powder (Sigma-Aldrich) was suspended in phosphate-buffered saline (10 mg/mL), filtered with 40-μm sterile strainer, and autoclaved. Although mammalian cells lack the chitin synthase enzyme, it has been demonstrated that the formation of GlcNAc oligomers can occur in particular experimental conditions by HAS-1 enzyme (Semino et al., 1996; Yoshida et al., 2002). Accordingly, we incubated SH-SY5Y with increasing concentrations of GlcNAc and UDP-GlcNAc (Sigma-Aldrich) for 72 hours and confirmed that such treatment induced a dose-dependent neurotoxicity (Supplementary Fig. 1A); based on these findings, we adopted the previously published condition (5-mM GlcNAc and 150-μM UDP-GlcNAc) for the subsequent studies on N9, primary microglial or neuronal cultures, and SH-SY5Y, fibroblasts or slice cultures.

2.4. Immunofluorescence and confocal microscopy

We first assessed in vitro the specificity of the binding of Calcofluor (Sigma-Aldrich) to chitin/GlcNAc polymers or to Aβ fibrils. For this purpose, amyloid fibrils were prepared by diluting $A\beta_{1-42}$ peptide (Bachem, Bubendorf, Switzerland) in Me_2SO (100 μM in 10-mM HCl), shaking for 30 seconds and incubating at 37 °C for 24 hours (Stine et al., 2003). Chitin was dissolved in 1% citrate-phosphate buffer (pH 7.3) and diluted in 0.1-M Tris-HCl, pH 9.0. Chitin and Aβ were incubated in 96-well plate at 4 °C overnight, and Calcofluor was then added for 1 hour at room temperature (RT). The fluorescence intensity was measured by spectrophotometer (SFM 25; Kontron Instruments) (excitation 365 nm, emission 440 nm). Immunofluorescence assays were performed on both brain paraffin sections and cell cultures. Sections of human brains were treated with 0.2% Calcofluor in Tris/HCl (0.1 M, pH 9) for 1 hour at RT, as previously described (Castellani et al., 2005; Sotgiu et al., 2008); in addition, the presence of GlcNAc polymers was assessed by rhodamine-conjugated chitin-binding probe (CBP, 1:500; New England Biolabs, Ipswich, MA, USA) incubated at 4 °C overnight (Bakkers et al., 1997). Double immunostaining was performed using Congo Red (Electron Microscopy Sciences, Hatfield, PA, USA) or Thioflavine S to stain amyloid plaques. Sections were viewed with Zeiss Axiolab fluorescent microscope (Carl Zeiss, Oberkochen, Germany) and analyzed with AxioVision LE Rel. 4.5 software or TCS SP5 confocal scanner (Leica, Heerbrugg, Switzerland). Cell cultures were fixed in 4% paraformaldehyde and permeabilized with 0.5% Triton. After incubation with 20% normal serum (Vector Laboratories, Burlingame, CA, USA), they were incubated with primary antibodies at 4 °C overnight: anti-mouse CD11b mAb (1:100; Serotec, Oxford, UK) for microglia, polyclonal anti-βIII tubulin (1:250; Millipore, Billerica, MA, USA), anti-mannose receptor mAb (1:50, clone 5C11; Abcam, Cambridge, UK), and polyclonal anti-human tau (1:200; Dako, Glostrup, Denmark). After washing with phosphate-buffered

saline, appropriate fluorescein-conjugated secondary antibodies (Molecular Probes; Life Technologies Ltd, Paisley, UK) or biotinylated secondary antibodies followed by Streptavidin-Texas Red (Vector) were added. Mannan (2 mg/mL; Sigma-Aldrich) has been added for 48 hours. The omission of primary antibodies was used as a negative control. To assess the synaptic impairment induced by GlcNAc/UDP-GlcNAc (72 hours) on SH-SY5Y, cells were subjected to immunofluorescence for synaptophysin (clone SY38, Millipore, Billerica, MA, USA) and β-III tubulin. The total fluorescence measurement (corrected total fluorescence [CTFC]) of synaptophysin signal was performed with Image J software. Images were taken with the same acquisition parameters. Integrated density was measured for each cell, and a similar area without fluorescent was measured and used for background subtraction. CTFC was calculated for each cell following the formulation: CTFC = integrated density − (area of selected cell × mean fluorescence of background readings).

2.5. Electron microscopy

N9 microglial cells incubated with chitin (1 mg/ml) or with 5-mM GlcNAc and 150-μM UDP-GlcNAc for 48 hours were evaluated by transmission (transmission electron microscopy [TEM], EM109; Zeiss) or scanning electron microscopy (DSM 950; Zeiss). For TEM, cells were then centrifuged at 150× *g*, washed, and fixed with 1.25% glutaraldehyde and 0.5% paraformaldeyde in phosphate buffer for 1 hour at 4 °C and postfixed in osmium tetraoxide for 2 hours at 4 °C. Pellets were subsequently dehydrated in acetone and included in Spurr resin. For scanning electron microscopy, cells were treated as mentioned previously and fixed to stubs with colloidal silver, spattered with gold with a MED 010 coater.

2.6. Assessment of cytotoxicity, proliferation, and activation

To evaluate the cytotoxic effect on β-III tubulin$^+$ neurons, CD11b$^+$ microglia, and fibronectin$^+$ fibroblasts, cells were counted on 10 random fields at 20× after treatment with chitin (1 mg/mL), 5-mM GlcNAc and 150-μM UDP-GlcNAc, 5-mM GlcNAc or 150 μM UDP-GlcNAc alone, chitosan, or 50-μg/mL oligomeric β amyloid (fragment Aβ_{25-35}; Bachem) (Brureau et al., 2013; Do et al., 2014). Experiments were performed in triplicate, and cells were blindly counted by 2 independent investigators. The cellular activation of N9 cells and the cytotoxic effect on SH-SY5Y were assessed by 3-(4,5-dimethylthiazol-2-yl)-2,5-diphenyltetrazolium bromide (MTT) assay; briefly, after treatment, cells were seeded into a flat bottom 96-well plate and incubated with 10-μL MTT solution (Cell proliferation Kit I; Roche Diagnostics GmbH, Penzberg, Germany) for 4 hours at 37 °C. Absorbance was measured at 550 nm after 24 hours with a spectrophotometer (BioRad Laboratories, Milano, Italy). The production of cytokines by N9 cells after the different treatments was assessed in their supernatants at 2 different time points (18 and 72 hours) by commercial assays (Milliplex Kit MCYTOMAG-70K-15 mouse; Merck Millipore) that measure granulocyte colony-stimulating factor (G-CSF), granulocyte-macrophage CSF, interferon γ, interleukin (IL)-1α, IL-1β, IL-2, IL-4, IL-5, IL-6, IL-7, IL-10, IL-12 (p40), IL-12 (p70), IL-17, and tumor-necrosis factor α (TNFα). Cytokine concentration was automatically calculated by Milliplex software using a standard curve derived from a recombinant cytokine.

The proliferation of N9 cells before and after treatments was assessed by adding 10-μM BrdU (Sigma-Aldrich) for 4 hours; cells were then fixed with methanol for 10 minutes and treated with 2N HCl and then with $Na_2B_4O_7$ (0.1 M, pH 8.5). Triple immunofluorescence was performed for CD11b and BrdU, whose signals were detected with secondary antibodies conjugated with Streptavidin Texas Red (Vector) and anti-mouse Alexa 488 (Molecular Probes) and the nuclear marker DAPI (Abbott Molecular, Inc, Abbott Park, IL, USA). The rate of mitotic activity was calculated dividing the number of BrdU$^+$ nuclei for the total number of cells.

2.7. Mass spectrometry analysis

To prepare cell extracts for mass spectrometry analysis, SH-SY5Y neuroblastoma and N9 microglial cell lines were cultured up to confluence and treated or not with 5-mM GlcNAc and 150-μM UDP-GlcNAc or with 5-mM GlcNAc alone for 48 hours. Cells were homogenized in liquid nitrogen and then placed at −80 °C. The powder was dissolved in 5 volumes of extraction solvent (water and methanol 4:1, vol/vol), sonicated at 40 kHz for 5 minutes, added with 5 volumes of water, and centrifuged twice at 12,000 rpm for 10 minutes. Supernatant were filtered (0.2-μm pore filters; Minisart RC 4), collected, and stored at −20 °C or immediately analyzed by reversed-phase high-performance liquid chromatography-mass spectrometry (HPLC-MS). For the reverse-phase HPLC-electrospray ionization-MS analyses, molecules were separated trough a Beckman Coulter Gold 127 HPLC System (Beckman Coulter, Fulleton, CA, USA) equipped with a C18 guard column (7.5 × 2.1 mm) and an analytical Alltima HP C18 column (150 × 2.1 mm and particle size, 3 μm) (Alltech Associates Inc, Deerfield, IL, USA). Two solvents were used for chromatographic elution: solvent A (94.5% H_2O, 5% acetonitrile, and 0.5% formic acid) and solvent B (100% acetonitrile). A solvent gradient was established from 0% to 2% B in 1 minute, isocratic at 2% for 3 minutes, from 2% to 6% B in 1 minute, isocratic at 6% for 5 minutes, and from 6% to 80% B in 3 minutes. Each sample was analyzed in duplicate, with 50-μL injection volumes and 25-minute equilibration between samples. The flow rate was set at 200 μL per minute. The HPLC system was coupled online with a Bruker ion trap mass spectrometer Esquire 6000, equipped with electrospray ionization. The mass spectrometer was set to perform the analysis in a positive ionization mode, and data were obtained setting a target mass of 1200 m/z, scan range of 50–2500 m/z, nebulizing gas at 50 psi at 350 °C, and a flux of 10 L/minute for the drying gas. For the chitin-like molecule identification, the instrument was set in fragmented positive ion modality reaching up to MS^3 fragmentation steps with fragmentation amplitude of 1V. The data were collected using the Bruker Daltonics Esquire 5.2-Esquire Control software and processing using the Bruker Daltonics Esquire 5.2-Data Analysis 3.2 software (Bruker Daltonics GmbH, Bremen, Germany). The fragmentation spectra of putative identified molecules were compared with the standard's fragmentation patterns.

2.8. Organotypic slice cultures

The hippocampal slices were obtained from 8- to 12-week-old C57BL/6 male mice killed by decapitation. The temporal lobes were cut into 350-μm-thick slices with vibratome. The hippocampal slices were then cultured for immunoblotting in MEM media (Corning) and treated with 5-mM GlcNAc and 150-μM UDP-GlcNAc or 50-μg/mL Aβ_{25-35} for 1 week. Slices were then homogenized in RIPA buffer containing protease inhibitors (Roche Diagnostics). After 2 hours at 4 °C, homogenates were centrifuged at 4000 rpm to discard cellular debris. Protein content was determined by Bradford Assay (Sigma-Aldrich). Protein lysates were diluted in Laemli buffer, boiled at 90 °C for 5 minutes, and then resolved by 12% sodium dodecyl sulfate-polyacrylamide gel electrophoresis. Proteins were transferred onto the nitrocellulose membrane (Bio-Rad), which were blocked with Tris-buffered saline and 0.1% Tween 20% and 10%

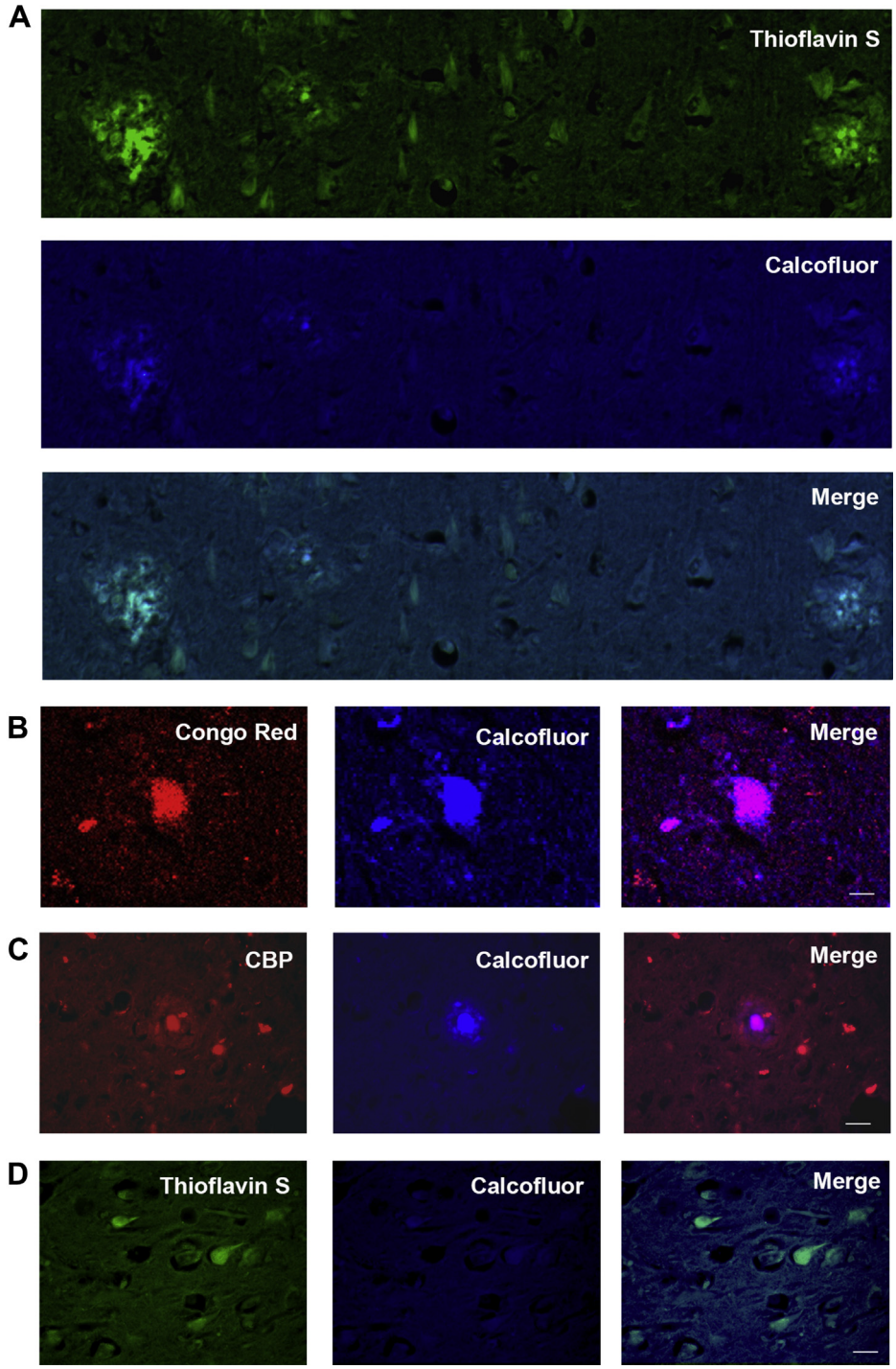

Fig. 1. *N*-acetylglucosamine polymers are present in amyloid plaques in sporadic Alzheimer's disease (AD). (A–C) Double staining shows colocalization of Calcofluor with Thioflavine S (A), Congo Red (B) and chitin-binding probe (C) in the vast majority of amyloid plaques from sporadic AD brains. (D) No Calcofluor signal has been observed on neurofibrillary tangle, evidenced by Thioflavin S staining. Bar: 20 μm.

nonfat dry milk (GE-Healthcare). Membranes were then incubated at 4 °C overnight with the following primary antibodies: syntaxin (Abcam), synaptophysin (Millipore), βIII tubulin, and actin (Sigma-Aldrich). Appropriate secondary IgG HRP-conjugated (GE Healthcare) was added for 1 hour, and chemiluminescent detection was performed with ECL Plus advanced (Amersham and GE Healthcare). Quantitative analysis of the signal obtained was performed by Image J software (National Institutes of Health).

2.9. Electrophysiology

Field excitatory postsynaptic potentials (fEPSPs) were recorded in acute hippocampal slices from 8- to 12-week-old C57BL/6 male mice. Animals were treated according to the guidelines of Animal Ethical Committee of the University of Verona: anesthetized by ether inhalation, perfused with ice-cold dissection media, and the cerebral hemispheres removed. Hippocampal

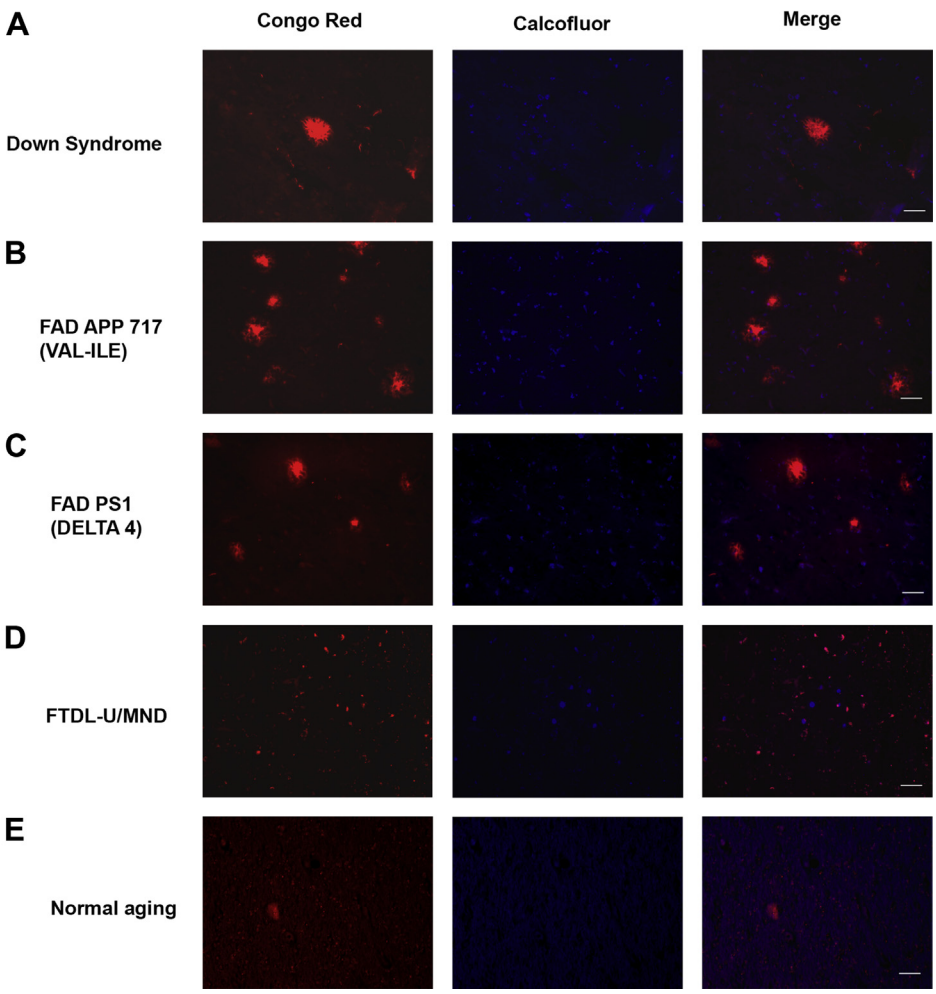

Fig. 2. *N*-acetylglucosamine (GlcNAc) polymers are absent in amyloid plaques in familiar Alzheimer's disease (AD). (A–C) Double staining with Congo Red and Calcofluor fails to show any GlcNAc deposit within amyloid plaques in familiar AD, such as Down syndrome (A) or AD with mutations in APP (B) or presenilin 1 (C) genes. No staining with either Congo Red or Calcofluor is seen in frontotemporal degeneration (D). The sporadic Congo Red$^+$ amyloid plaques detectable in nondemented age-matched controls show no evidence of GlcNAc deposits by Calcofluor (E), apart faint unspecific nuclear staining. Bar: 20 μm.

coronal slices (350 μm thick) were cut in ice-cold dissection media and subsequently allowed to recover at 32 °C for 1 hour in artificial cerebrospinal fluid (ACSF). Slices were then incubated with 5-mM GlcNAc and 150-μM UDP-GlcNAc for 3 and 5 hours at 32 °C. Control slices received GlcNAc, UDP-GlcNAc, or ACSF. Finally, slices were transferred in a recording chamber and perfused at 2–3 mL per minute with ACSF at RT. When needed, $A\beta_{25-35}$ (50 μg/mL) was added during the recording. Axons of the Schaffer collateral pathway were stimulated with a borosilicate glass electrode (thin wall, 30–60 μm tip diameter; W.P.I., Sarasota, FL, USA) filled with the bathing solution. The evoked fEPSPs were recorded with a borosilicate glass electrode filled with bathing solution (standard wall, 1–2 MΩ resistance; Warner Instr, Hamden, CT, USA) and placed in the stratum radiatum at the CA1 level, 100–300 μm from the stimulating electrode. fEPSPs were amplified (×100), filtered (2 kHz), and recorded with an Axopatch 200B amplifier (Molecular Devices, Sunnyvale, CA, USA), digitized at 20 kHz (Digidata 1322A; Molecular Devices) and acquired with pClamp 9.2 software. Data were analyzed with Clampfit 9.2 software (Molecular Devices). Typically, the evoked fEPSPs reached stable amplitude within 20–40 minutes of low-frequency stimulation (0.05 Hz). After this period, a 20-minute baseline recording was obtained. Subsequently, a long-term potentiation (LTP)–inducing high-frequency stimulation (HFS) protocol was applied, and its effect measured afterward with low-frequency stimulation for 60 minutes. HFS consisted of a train of stimuli at 100 Hz (1-second train duration) repeated 4 times every 20 seconds. Baseline fEPSPs amplitude was set at 40%–50% of their maximal amplitude. The magnitude of LTP was measured during the last 10 minutes of recording and expressed as the mean (±standard error of the mean) fEPSP slope (10%–90% of the initial segment) relative to the average baseline. When necessary, 4-(3-phosphonopropyl) piperazine-2-carboxylic acid (10 μM) was applied in the recording chamber to block *N*-methyl D aspartate (NMDA)–type glutamate receptors. Paired pulse facilitation (PPF) was calculated from 2 fEPSPs separated by 50 ms as the ratio (±standard error of the mean) between the slope of the second event relative to the value of the first event.

2.10. Statistical analyses

Univariate analysis of variance and post hoc test with Bonferroni correction were applied for the evaluation of cellular toxicity or activation. All data in vitro represent results of 3 independent experiments. Data are expressed as the mean ± standard deviation.

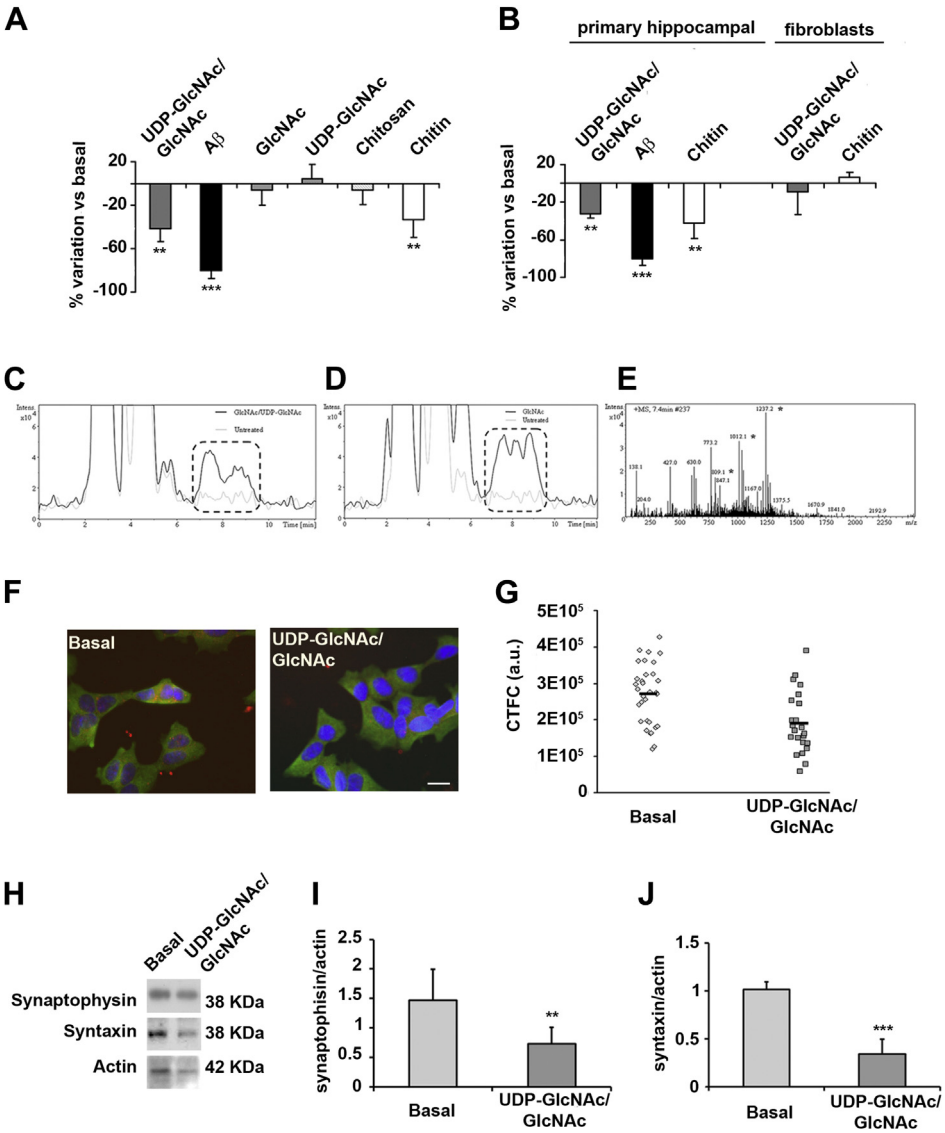

Fig. 3. Neurotoxicity by *N*-acetylglucosamine (GlcNAc) oligomers in cells and slice cultures. (A) Significant levels of cytotoxicity compared with basal conditions are observed on SH-SY5Y neuronal cultures exposed to 5-mM GlcNAc/150-μM uridine diphosphate (UDP)-GlcNAc, chitin fragments, or amyloid-β $(Aβ)_{25–35}$, but neither to GlcNAc or UDP-GlcNAc alone nor to chitosan. (B) Similar results are obtained in primary hippocampal neurons with 5-mM GlcNAc/150-μM UDP-GlcNAc, chitin fragments, or $Aβ_{25–35}$, whereas fibroblasts are resistant to either 5-mM GlcNAc/150-μM UDP-GlcNAc or chitin. (C and E) Chromatograms of human SH-SY5Y cell line. The box indicates the oligomers elution zone. (C) Chromatograms from cells treated (black line) or not (gray line) with GlcNAc/UDP-GlcNAc (C) or with GlcNac alone (D). (E) Mass spectrum at 7.4 minutes (within the peak highlighted in the box in C). The asterisks highlight 3 oligomers of m/z 809, 1012, and 1237, corresponding to 2, 3, and 4 residues of GlcNAc linked with a UDP, respectively (the last one was detected as sodium adduct). The fragmentation pattern of these 3 oligomers matches with that of UDP-GlcNAc standard (data not shown). (F and G) Triple staining for DAPI (blue), synaptophysin (red), and β-III-tubulin (green) shows a significant reduction of synaptophysin on SH-SY5Y treated with GlcNAc/UDP-GlcNAc. Integrated density of the signal for synaptophysin and its corrected total fluorescence (CTFC) value was measured for each cell. (H and J) The immunoblotting for synaptophysin and syntaxin on homogenates from slice cultures with or without treatment with GlcNAc/UDP-GlcNAc shows a significant decrease of both synaptophysin and syntaxin proteins, after normalization to actin levels.

Statistical analyses were performed using SPSS software, version 19 (IBM, Armonk, NY, USA). Electrophysiological data were analyzed with Student *t* test or 1-way analysis of variance. All reported *p* values were corrected for multiple comparisons, and a corrected *p* value of <0.05 was used to define statistical significance.

3. Results

3.1. GlcNAc polymers are present in sporadic but not FAD plaques

Deposits of GlcNAc polymers have been observed with Calcofluor in amyloid plaques present in the hippocampus and cerebral cortex of sporadic AD cases, with a clear colocalization with Congo Red or Thioflavine S (Fig. 1A and B). The strict colocalization of the signals of Congo Red/Thioflavine S and Calcofluor in amyloid plaques in sporadic AD prompted us to verify whether Calcofluor indeed bound GlcNAc deposits and was not because of unspecific binding to similar conformational (β sheets) epitopes. For this purpose, we first verified that Calcofluor signal colocalizes with the chitin-specific marker CBP (Fig. 1C). In addition, we assessed by spectrophotometer the specificity of Calcofluor for chitin particles ($p = 0.0008$, Supplementary Fig. 1B). Particular attention has been paid to the colocalization of signals for Calcofluor on neurofibrillary tangle, but we failed to detect any significant association (Fig. 1D).

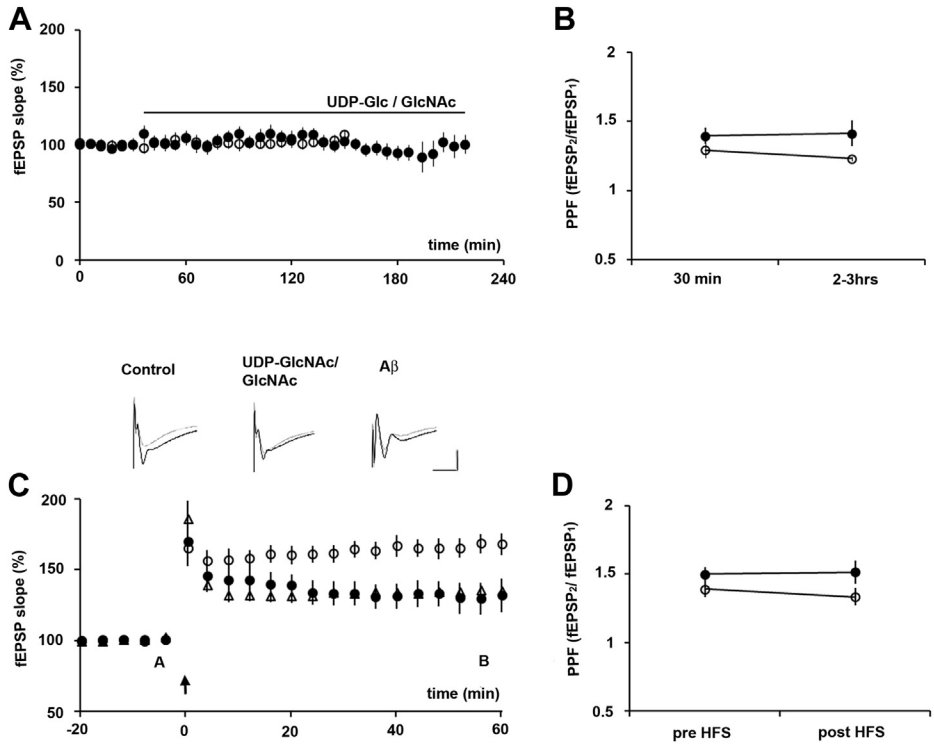

Fig. 4. *N*-acetylglucosamine (GlcNAc) affects long-term potentiation (LTP) of excitatory inputs in acute hippocampal slices. (A) Field excitatory postsynaptic potential (fEPSP) slopes are stable during prolonged recordings both in control (open dots, $n = 7$) and in the presence of GlcNAc/uridine diphosphate (UDP)-GlcNAc (black dots, $n = 5$). Stimulation frequency: 0.025 Hz; 9 successive responses grouped together and normalized to the mean value during the first 30 minutes. The horizontal bar indicates the duration of treatment. (B) Paired pulse facilitation (PPF) of fEPSP slopes during the first 30 minutes and at the end (2–3 hours) of the recordings (same experiments of A). Control: open dots; GlcNAc/UDP-GlcNAc–treated slices: black dots. No significant difference within each group and between the 2 groups. (C) Incubation with GlcNAc/UDP-GlcNAc (black dots) or amyloid-β $(A\beta)_{25-35}$ (open triangles) causes smaller LTP of fEPSP slopes compared with control (open dots). Test stimulation frequency: 0.05 Hz; 12 successive responses grouped together and normalized to the mean value during the first 20 minutes. Arrow marks the time of high-frequency stimulation (HFS) (100 Hz). Values 50 minutes after HFS: control = 165% ± 6%, $n = 11$; GlcNAc/UDP-GlcNAc = 131% ± 10%, $n = 10$, $p = 0.01$; $A\beta_{25-35}$ = 135%±3%, $n = 6$, $p = 0.002$. Insets show representative fEPSP recordings (averages of 20 successive responses) made at time A (gray lines) and B (black lines). Scale bars: 10 ms and 0.5 mV. (D) PPF of fEPSP slopes before and 50 minutes after HFS (same experiments of C). Control: open dots, $n = 9$; GlcNAc/UDP-GlcNAc–treated slices: black dots, $n = 9$. No significant difference within each group and between the 2 groups.

It is important to note that, at variance with the previous reports (Castellani et al., 2005), no signal for either Calcofluor or CBP was observed in amyloid plaques in all FAD cases and Down syndrome (Fig. 2A–C) and in frontotemporal dementia (without amyloid plaques) (Fig 2D), apart faint unspecific nuclear staining. Even more interesting was the study of age-matched nondemented individuals, where Calcofluor showed no signal in the sporadic Congo Red^+ amyloid plaques (Fig. 2E).

3.2. Oligomerization of GlcNAc induces neurotoxicity in cell cultures

The incubation with 5-mM GlcNAc and 150-μM UDP-GlcNAc induced a significant neuronal cell death on both the neuronal cell line SH-SY5Y (reduction of cell viability: 42%, $p = 0.005$) and primary hippocampal neurons (33%, $p = 0.006$) as evidenced by reduced cell counts (Fig. 3A and B, Supplementary Fig. 1D) and decrease of metabolic activity by MTT (Supplementary Fig. 1C), whereas no effect has been observed with chitosan or with GlcNAc and UDP-GlcNAc alone (Fig. 3A and B). The comparative analysis of cytotoxicity between GlcNAc oligomers and Aβ showed higher levels of neurotoxicity for the latter (Fig. 3A and B, SH-SY5Y, $p = 0.0002$; hippocampal neurons, $p = 0.0003$), but no additional or synergistic effect was observed with the coincubation of GlcNAc oligomers and Aβ (data not shown). Interestingly, the exposure to GlcNAc oligomers had no visible effect on fibroblasts (Fig. 3B), suggesting that such treatment induced a selective neuronal toxicity. In parallel, we assessed whether the incubation with GlcNAc and UDP-GlcNAc leads to the formation of chitin-like deposits, but we failed to detect any positive signal with either Calcofluor or CBP on neuronal cultures (data not shown). To explain the significant neurotoxicity in the absence of detectable GlcNAc deposits, we hypothesized that the incubation with GlcNAc and UDP-GlcNAc in neuronal cells may induce small GlcNAc oligomers (i.e., below the sensitivity of Calcofluor). To confirm such hypothesis, we used a highly sensitive technique, HPLC-MS, on cellular extracts of SH-SY5Y cells treated or not with GlcNAc and UDP-GlcNAc. The chromatograms showed specific peaks in samples not only treated with GlcNAc and UDP-GlcNAc but also after treatment with GlcNAc alone (Fig. 3C and D); these peaks included signals of at least 3 oligomers of GlcNAc (respectively with 2, 3, and 4 GlcNAc residues) linked to UDP (Fig. 3E).

3.3. Functional and structural synaptic impairments by GlcNAc oligomers

To assess whether GlcNAc oligomers exert any functional or structural effect on synapses, we employed hippocampal slices, an experimental setting where physiologic intercellular connections (between neurons and/or glial cells) are largely preserved. We first monitored fEPSPs evoked in stratum radiatum of CA1 hippocampal area in the presence of GlcNAc and UDP-GlcNAc and found no modification of their slope during 3 hours recordings (Fig. 4A). This result suggests that the basal synaptic transmission was not

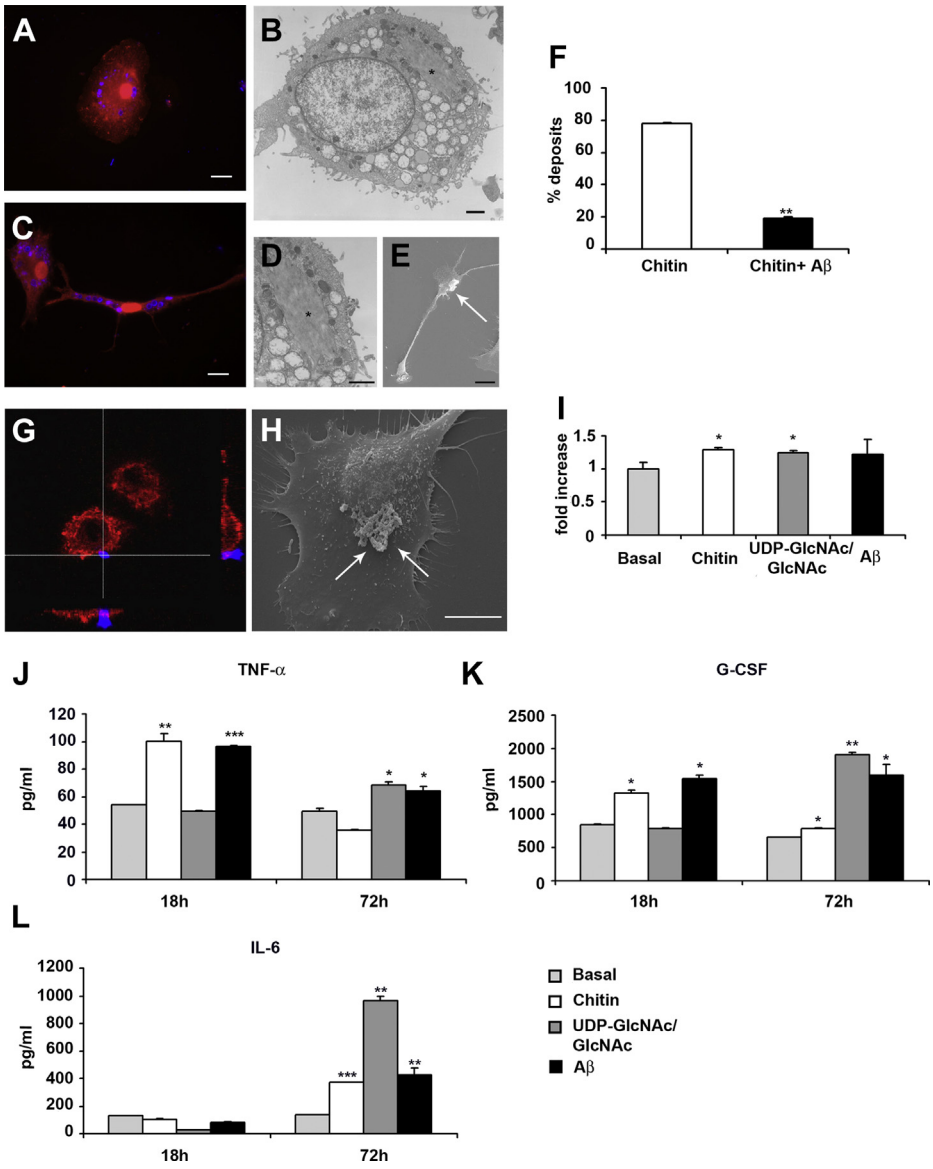

Fig. 5. Phagocytosis of chitin and endogenous production of *N*-acetylglucosamine (GlcNAc) polymers by microglia. (A–E) $CD11b^{+}$ (red) N9 cell line (A) and primary microglial culture (C) phagocytose small chitin fragments detected by Calcofuor (blue) and visible in their cytoplasm at the transmission electron microscopy (B and at higher magnification D) and standard error of the mean (SEM) (E) indicated by the arrows. Bars: A, C, and E: 20 μm; B and D: 1 μm. (F) The process of chitin phagocytosis by N9 cells is strongly inhibited by the concomitant presence of amyloid-β (Aβ). (G and H) $CD11b^{+}$ (red) N9 cells exposed to 5-mM GlcNAc/150-μM uridine diphosphate (UDP)-GlcNAc for 72 hours produce $Calcofluor^{+}$ (blue) deposits visible at the confocal microscopy (G) or SEM (arrows in H) in close proximity to plasma membrane and almost extruded in the extracellular space. Bar: (H) 10 μm. (I) Activation of microglia measured by 3-(4,5-dimethylthiazol-2-yl)-2,5-diphenyltetrazolium bromide assay; compared with basal conditions, a significant increase is observed after exposure for 72 hours to 5-mM GlcNAc/150-μM UDP-GlcNAc or chitin. (J–L) A significant increase of the cytokines tumor-necrosis factor α (TNFα), granulocyte colony-stimulating factor (G-CSF), and interleukin (IL-6) has been documented after 18 hours of incubation with chitin and amyloid-β (Aβ), whereas such effect with GlcNAc/UDP-GlcNAc was visible after 72 hours, according to kinetic of chitin-like particle formation.

acutely affected. Accordingly, also the presynaptic vesicle release probability was not affected, with the paired-pulse ratio of fEPSP slope being stable throughout the recordings (Fig. 4B). We then investigated the influence of GlcNAc and UDP-GlcNAc on synaptic plasticity looking at LTP induced by HFS. We found a 52% LTP reduction relative to control ($p = 0.007$) (Fig. 4C), a result in line with the neurotoxic effect observed in cell and slice cultures. No modification of PPF was observed both in control and in GlcNAc/UDP-GlcNAc–treated slices before and after HFS (Fig. 4D), in line with the widely described postsynaptic site of LTP expression in CA1 hippocampal area and also with a postsynaptic site of action of GlcNAc and UDP-GlcNAc. A negative influence on synaptic plasticity has been previously described in great detail for Aβ oligomers acutely applied to hippocampal slices (Chen et al., 2000; Haass and Selkoe, 2007; Koffie et al., 2011; Lambert et al., 1998; Nomura et al., 2005; Raymond et al., 2003; Shankar et al., 2008; Townsend et al., 2006; Turner et al., 2003). We thus repeated the experiment in the presence of $A\beta_{25-35}$ and found that LTP was similarly reduced (47% relative to control, $p = 0.002$) (Fig. 4C). The negative influences of GlcNAc/UDP-GlcNAc and that of $A\beta_{25-35}$ on LTP expression seemed to occlude each other. In fact, when recording in the presence of GlcNAc, UDP-GlcNAc, and $A\beta_{25-35}$, the degree of LTP reduction was of the same amount as that observed with only GlcNAc/UDP-GlcNAc or only $A\beta_{25-35}$ (46%, $p = 0.0009$;

LTP value 125% ± 7.6% of baseline fEPSP slope, $n = 6$). In partial discrepancy with our results on toxicity in primary cultured neurons (Fig. 3), LTP was also reduced when adding only GlcNAc or UDP-GlcNAc in the bath (59%, $p = 0.001$ and 41%, $p = 0.04$, respectively; LTP value with GlcNAc: 127% ± 5.8%, $n = 6$; with UDP-GlcNAc: 138% ± 10.1%, $n = 8$). Finally, the block of NMDA receptors with 4-(3-phosphonopropyl) piperazine-2-carboxylic acid completely prevented the expression of LTP (94.6% ± 6.1% of baseline fEPSP slope, $n = 4$), in accordance with the literature.

We then assessed the effect of the longer incubation of GlcNAc/UDP-GlcNAc in both SH-SY5Y and in organotypic hippocampal cultures to evaluate the occurrence of structural synaptic damage. In the first set of experiments, we found that the exposure of SH-SY5Y to GlcNAc/UDP-GlcNAc for 72 hours induced a significant reduction of the number of synatpophysin$^+$ signal (Fig. 3F and G). These results were then confirmed on hippocampal slices treated or not with GlcNAc/UDP-GlcNAc for up to 7 days and analyzed by immunoblotting with the synaptic markers synaptophysin and syntaxin. We observed a significant downregulation of both synaptic markers (Fig. 3H and J, synaptophysin, $p = 0.01$; syntaxin, $p = 0.0002$). Similarly, a chronic treatment of organotypic cultures with Aβ oligomers is known to cause a synapse loss (Koffie et al., 2011; Shankar et al., 2007, 2008; Turner et al., 2003).

3.4. Phagocytosis of chitin and polymerization of GlcNAc in microglia in vitro

We have previously shown that Calcofluor$^+$ deposits not only are present in amyloid plaques but are also detectable within the cytoplasm of surrounding microglia (Sotgiu et al., 2008). This finding prompted us to investigate whether these deposits result from the phagocytosis of extracellular GlcNAc polymers or are first produced by microglial cells and eventually released in the extracellular space. For this purpose, we first added chitin particles to N9 cell line, primary microglial cultures, or fibroblasts for 48 hours. Calcofluor$^+$ and CBP$^+$ staining and electron microscopy analysis confirmed the ability of N9 microglial cells (Fig. 5A–E) and fibroblasts (data not shown) to phagocytose small chitin fragments. In this regard, we demonstrated that chitin phagocytosis is mediated by the binding to the mannose receptor present on microglia because its blocking with mannan induced a 3-fold reduction ($p = 0.009$) of chitin uptake by microglia (Supplementary Fig. 1E and F). Interestingly, we found that chitin phagocytosis was strikingly inhibited by the presence of Aβ in the culture medium (Fig. 5, F, $p = 0.002$). These experiments clearly demonstrate the ability of microglia to phagocytose extracellular chitin small fragments and that the process is significantly inhibited by the concomitant presence of Aβ.

We then verified the ability of microglial cells and fibroblasts to produce GlcNAc polymers, similarly to neurons. N9 cell line, primary microglial cultures, or fibroblasts were incubated with 5-mM GlcNAc and 150-μM UDP-GlcNAc for 72 hours and such treatment led to the formation of Calcofluor$^+$ and CBP$^+$ polymers that were detectable in their cytoplasm. In addition, the analysis by confocal and electron microscopy evidenced the presence of Calcofluor$^+$ and CBP$^+$ deposits in close proximity of the plasma membrane of microglia and in the extracellular space (Fig. 5G and H). Moreover, the accumulation of GlcNAc polymers was confirmed by HPLC-MS in N9 cells treated with GlcNAc and UDP-GlcNAc but not with GlcNAc alone (data not shown).

3.5. GlcNAc polymers induce the activation of microglia

We finally verified the biological changes triggered in microglia by the presence of GlcNAc polymers (deriving either from phagocytosis or endogenous synthesis). For this purpose, we assessed the metabolic activity of microglia by MTT and cytokine profile. The presence of GlcNAc polymers in the cytoplasm significantly increased the metabolic activity of microglia to levels comparable with the exposure to Aβ (Fig. 5I, GlcNAc/UDP-GlcNAc, $p = 0.04$) (Da Silva et al., 2008; Lee et al., 2008; Meda et al., 1995; Nishimura et al., 1984). Such metabolic activation was accompanied by increased production of the pro-inflammatory cytokines TNFα, G-CSF, and IL-6, whereas all the other cytokines investigated showed no significant changes after treatments (data not shown). In particular, incubation of N9 cells with both chitin and Aβ for 18 hours significantly increased the levels of TNFα and G-CSF; in line with the kinetic of chitin-like particle formation with GlcNAc/UDP-GlcNAc, we observed a significant increased of all the 3 cytokines after 72-hour exposure (Fig. 5J–L). No significant change in the proliferation rate of microglia was found in any experimental condition (data not shown).

4. Discussion

In the present study, we provide evidence that polymerization of GlcNAc represents a novel pathogenic pathway that, together with Aβ and tau, may contribute to neuronal damage in sporadic AD. According to the "amyloid cascade hypothesis" (Abbott, 2008; Haass and Selkoe, 2007; Koffie et al., 2011; Querfurth and La Ferla, 2010; Turner et al., 2003), the accumulation of Aβ triggers a complex cascade with eventual synaptic and neuronal injury and progressive dementia. This hypothesis well explains the biological events occurring in FAD patients with mutations involving Aβ-related molecules and have been confirmed in transgenic mice carrying the same mutations (Chapman et al., 1999; Games et al., 1995; Hsiao et al., 1996; Ittner et al., 2010; Lewis et al., 2001; Oakley et al., 2006; Oddo et al., 2003). However, the translational relevance of such information to sporadic AD was surprisingly far below the expectancy. Intriguing in this regard were the results from the recent clinical trials aiming to decrease Aβ burden in sporadic AD, where the reduction of cerebral amyloid plaques was not accompanied by substantial clinical benefits (Doody et al., 2014; Holmes et al., 2008; Lemere and Masliah, 2010; Salloway et al., 2014). Although a number of explanations have been claimed for this (lack of) result, the possibility that FAD and sporadic AD differ in terms of fine pathogenic mechanisms has to be considered because of the complex scenario of sporadic AD where multiple factors (besides Aβ-dependent events) contribute to the neuronal damage. Thus, in the contest of sporadic AD, these considerations strongly suggest the need to consider the contribution of other cytotoxic pathways not yet explored. It is widely known that, beside Aβ, other molecules are present in amyloid plaques (O'Callaghan et al., 2008; Timmer et al., 2010; Van Horssen et al., 2003).

We focused our attention on GlcNAc polymers as potential pathogenic players in sporadic AD. We and others have previously shown that amyloid plaques of AD brains are recognized by Calcofluor (Castellani et al., 2005; Sotgiu et al., 2008), which binds the insoluble polymers of GlcNAc with β-sheet conformation (Castellani et al., 2007; Muzzarelli, 1997); in addition, the enzyme that usually degrades chitin, chitotriosidase, has been found to be significantly increased in plasma of sporadic AD patients (Barone et al., 2007; Sotgiu et al., 2007). Although mammals lack chitin synthase, it has been demonstrated that GlcNAc oligomers can be obtained by the HAS-1 enzyme in the presence of excess of UDP-GlcNAc (Semino et al., 1996; Yoshida et al., 2002). We first compared the staining with Calcofluor and CBP (both specifically binding GlcNAc polymers) in brain sections from sporadic and genetic AD to assess whether the composition of the amyloid plaques differ regarding the presence of GlcNAc polymers. Indeed,

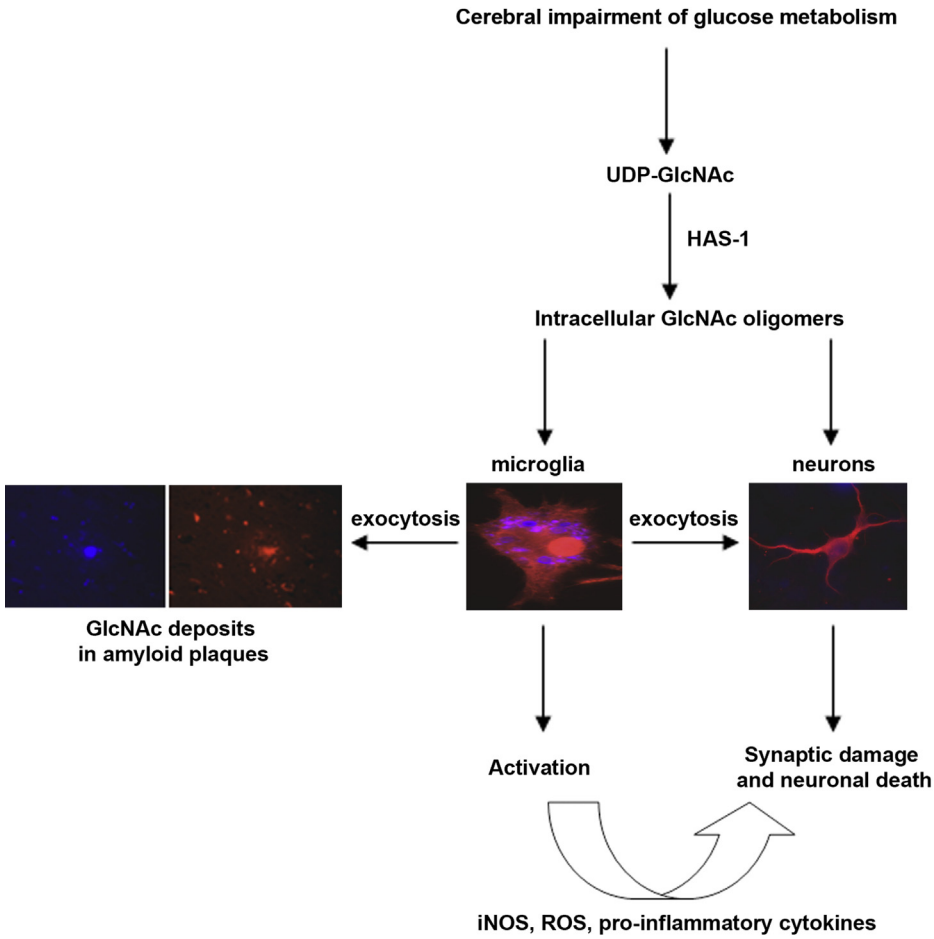

Fig. 6. Schematic representation of the possible role of *N*-acetylglucosamine (GlcNAc) oligomers/polymers in the pathogenesis of Alzheimer's disease. The cerebral impairment of glucose metabolism may shift its utilization to the hexosamine pathway, whose end product is uridine diphosphate (UDP)-GlcNAc. The excess of GlcNAc and UDP-GlcNAc, possibly through hyaluronan synthase-1 (HAS-1), leads to insoluble GlcNAc oligomers in neurons (where it induces synaptic damage and cell death) and in microglia. In the latter, intracellular deposits of GlcNAc activate microglia and are released (exocytosis) in the extracellular space where it accumulate in amyloid plaques and contribute to neuronal damage either directly or through the production of pro-inflammatory cytokines, inducible nitric oxide (iNOS) and superoxygen radicals (reactive oxygen species [ROS]).

positive signals were visible with both techniques and colocalized with Congo Red/Thioflavine S on amyloid plaques only in sporadic AD brains, whereas Congo Red^{+} plaques from FAD brains and nondemented age-matched controls did not apparently contain GlcNAc polymers.

We then assessed whether mammalian cells were indeed able to form GlcNAc polymers in vitro in neurons and microglia. Adopting a previously described protocol (Semino et al., 1996; Yoshida et al., 2002), we indeed found evidence by HPLC mass of GlcNAc oligomerization in the cytoplasm of both neurons and microglia. GlcNAc oligomers in neurons did not give rise to intracellular or extracellular deposits detectable with Calcofluor or CBP, possibly because of their small size.

We then investigated the biologic effects of GlcNAc oligomers in 2 distinct in vitro models assessing short- and long-time exposures in terms of functional (synaptic) and structural neuronal damage. We present functional evidence of impaired synaptic plasticity caused by GlcNAc oligomers. In fact, by recording fEPSP in hippocampal slices in the presence of GlcNAc/UDP-GlcNAc, we showed that LTP expression was affected at a level comparable with Aβ oligomers. It is well known that the acute exposure of brain slices to Aβ oligomers impedes LTP and favors long-term depression (Chen et al., 2000; Lambert et al., 1998; Nomura et al., 2005; Raymond et al., 2003; Shankar et al., 2008; Townsend et al., 2006). In particular, Aβ oligomers interfere with synaptic NMDA receptors reducing calcium current flow (Nomura et al., 2005; Snyder et al., 2004; Raymond et al., 2003; Shankar et al., 2007), whereas activating the extrasynaptic NMDA receptors (Li et al., 2009, 2011). As a final outcome, LTP is inhibited and long-term depression is promoted (Koffie et al., 2011; Turner et al., 2003). Finally, the observation that fEPSPs were stable when evoked at low frequency for several hours in the presence of GlcNAc/UDP-GlcNAc also indicates that the reduction of LTP is not because of a partial occlusion of synaptic potentiation. In line with these experiments, we observed that the exposure of GlcNAc oligomers for 2–3 days induced a selective dose-dependent cytotoxicity of neuronal cells, but not on other cells, such as fibroblasts and microglia (see subsequently), suggesting that GlcNAc oligomers induced a selective neuronal toxicity, almost as severe as Aβ. In analogy with Aβ, our results indicate a length-dependent effect of GlcNAc polymers, with shorter molecules being more neurotoxic. We paid particular attention to the effect of the deacetylated form of GlcNAc, chitosan, which has a number of commercial and biomedical use (e.g., biopesticide, fungal infections, bandages to reduce bleeding and scars, and soluble dietary fiber), but we failed to demonstrate any neurotoxicity. In addition, we evaluated the effect of GlcNAc oligomers in organotypic slice cultures, where the physiologic intercellular connections and synapses are largely preserved. Indeed, by

means of immunoblotting, we found that GlcNAc oligomers induced a significant reduction of syntaxin and synaptophysin, which is indicative of a synaptic structural derangement. In parallel with the effect induced by the intracellular formation of GlcNAc oligomers, we demonstrated that also extracellular GlcNAc polymers (mimicked here by small chitin fragments) exerted a significant neurotoxic effect to levels comparable with endogenous GlcNAc oligomers.

The second pathogenic aspect addressed in this study concerned the effect of GlcNAc polymers on microglia, as demonstrated for Aβ (Meda et al., 1995). We first set up a series of experiments to assess whether such cytoplasmic accumulation derived from the phagocytosis of extracellular deposits or was the result of endogenous production, as shown for neurons. For this purpose, we exposed microglial cells (both N9 cell line and primary cultures) to small chitin particles. We indeed confirmed the ability of microglia to phagocytose chitin particles through the mannose receptor, with a consequent increase of metabolic activity, as reported for macrophages (Shibata et al., 1997). Interesting in view of the pathogenetic implication for AD was the finding that the coincubation with Aβ significantly inhibited chitin phagocytosis. We finally explored the ability of microglia to produce GlcNAc polymers in vitro and their biological consequences. After incubation with GlcNAc/UDP-GlcNAc, we found Calcofluor^{+} and CBP^{+} signals within microglial cells, sometimes in close proximity of the plasma membrane and in the extracellular space. As shown with chitin fragments and Aβ, the endogenous formation of GlcNAc polymers after 72 hours activated microglia cells with elevated production of the pro-inflammatory cytokines TNFα, G-CSF, and IL-6. Thus, despite the increased levels of the chitin-degrading enzyme chitotriosidase found in AD patients (Barone et al., 2007; Sotgiu et al., 2007), the production and the deposition of extracellular deposits of GlcNAc polymers in sporadic AD by microglial cells may contribute to neurotoxicity (Fig. 6).

An important question that remains open concerns the condition(s) predisposing to GlcNAc polymerization in sporadic AD brains. One possibility may be a defective degradation of GlcNAc polymers secondary to impaired activity of chitotriosidase. In this regard, a rather common polymorphism among Caucasians (5%–6%, Piras et al., 2007) is characterized by abolished chitotriosidase activity (Boot et al., 1998). Although additional experiments are needed, our previous finding of increased levels of chitotriosidase in sporadic AD (Sotgiu et al., 2007) argues against such hypothesis. Alternatively, a possible explanation foresees a local hyperproduction of GlcNAc polymers that overcome the physiological degradation by chitotriosidase, possibly because of glucose metabolism derangement in neurons as suggested by a number of functional and pathologic evidences (Arvanitakis et al., 2004; Ishii et al., 1996, 1998; Piert et al., 1996; Shah et al., 2012; Simpson and Davies, 1994; Simpson et al., 1994). As a consequence, such glucose derangement may create the conditions of GlcNAc polymerization, considering that GlcNAc is the end product of the hexosamine pathway (Love and Hanover, 2005; Shah et al., 2012). In addition, the increased glucose utilization in hexosamine rather than in glycolytic pathway may derive from genetic mutations or acquired influences on key enzymes regulating GlcNAc metabolism. In this regard, it is interesting to note that a candidate locus for late-onset AD maps to a region of chromosome 10 near to the gene encoding O-GlcNAcase and insulin degrading enzyme (Bertram et al., 2000; Nowotny et al., 2005).

5. Conclusions

Taken together, our in vitro experiments recapitulate several histochemical findings observed in vivo in human sporadic AD brains (Fig. 6). In fact, Calcofluor^{+} and CBP^{+} deposits have been documented in the extracellular space (i.e., amyloid plaques) and in the cytoplasm of microglia but not in neurons both in vitro and in situ. In light of these considerations, future therapeutic strategies for sporadic AD should take into account the complexity of the disease with the aim not only to reduce the amyloid burden but also to modulate the formation of GlcNAc polymers and/or the inhibition of key steps in the biosynthesis of UDP-GlcNAc.

Disclosure statement

The authors have no conflicts of interest to disclose.

Acknowledgements

We thank the MRC London Brain Bank for Neurodegenerative disease for providing central nervous system samples from familiar AD patients. We are grateful to Riccardo Muzzarelli and Elena Bazzoli for their stimulating discussion on chitin biology and to Salvatore Monaco, Sergio Ferrari, and GianLuigi Zanusso for their helpful discussion. We thank Paolo Bernardi and Alessandra Danese for their helpful technical support. The authors declare no competing financial interests.

Appendix A. Supplementary data

Supplementary data associated with this article can be found, in the online version, at http://dx.doi.org/10.1016/j.neurobiolaging.2014.12.033.

References

Abbott, A., 2008. The plaque plane. Nature 456, 161–164.
Arvanitakis, Z., Wilson, R.S., Bienias, J.L., Evans, D.A., Bennett, D.A., 2004. Diabetes mellitus and risk of Alzheimer disease and decline in cognitive function. Arch. Neurol 61, 661–666.
Bakkers, J., Semino, C.E., Stroband, H., Kijne, J.W., Robbins, P.W., Spaink, H.P., 1997. An important developmental role for oligosaccharides during early embryogenesis of cyprinid fish. Proc. Natl. Acad. Sci. U.S.A 94, 7982–7986.
Barone, R., Sotgiu, S., Musumeci, S., 2007. Plasma chitotriosidase in health and pathology. Clin. Lab 53, 321–333.
Bertram, L., Blacker, D., Mullin, K., Keeney, D., Jones, J., Basu, S., Yhu, S., McInnis, M.G., Go, R.C., Vekrellis, K., Selkoe, D.J., Saunders, A.J., Tanzi, R.E., 2000. Evidence for genetic linkage of Alzheimer's disease to chromosome 10q. Science 290, 2302–2303.
Boot, R.G., Renkema, G.H., Verhoek, M., Strijland, A., Bliek, J., de Meulemeester, T.M., Mannens, M.M., Aerts, J.M., 1998. The human chitotriosidase gene. Nature of inherited enzyme deficiency. J. Biol. Chem 273, 25680–25685.
Brownlee, M., 2001. Biochemistry and molecular cell biology of diabetic complication. Nature 414, 813–820.
Brureau, A., Zussy, C., Delair, B., Ogier, C., Ixart, G., Maurice, T., Givalois, L., 2013. Deregulation of hypothalamic-pituitary-adrenal axis functions in an Alzheimer's disease rat model. Neurobiol. Aging 34, 1426–1439.
Castellani, R.J., Siedlak, S.L., Fortino, A.E., Perry, G., Ghetti, B., Smith, M.A., 2005. Chitin-like polysaccharides in Alzheimer's disease brains. Curr. Alzheimer Res 2, 419–423.
Castellani, R.J., Perry, G., Smith, M.A., 2007. The role of novel chitin-like polysaccharides in Alzheimer disease. Neurotox Res 12, 269–274.
Chapman, P.F., White, G.L., Jones, M.W., Cooper-Blacketer, D., Marshall, V.J., Irizarry, M., Younkin, L., Good, M.A., Bliss, T.V., Hyman, B.T., Younkin, S.G., Hsiao, K.K., 1999. Impaired synaptic plasticity and learning in aged amyloid precursor protein transgenic mice. Nat. Neurosci 2, 271–276.
Chen, Q.S., Kagan, B.L., Hirakura, Y., Xie, C.W., 2000. Impairment of hippocampal long-term potentiation by Alzheimer amyloid β-peptides. J. Neurosci. Res 60, 65–72.
Da Silva, C.A., Hartl, D., Liu, W., Lee, C.G., Elias, J.A., 2008. TLR-2 and IL-17A in chitin-induced macrophage activation and acute inflammation. J. Immunol 181, 4279–4286.
Do, T.D., Economou, N.J., Chamas, A., Buratto, S.K., Shea, J.E., Bowers, M.T., 2014. Interactions between amyloid-β and Tau fragments promote aberrant aggregates: implications for amyloid toxicity. J. Phys. Chem. B 118, 11220–11230.
Doody, R.S., Thomas, R.G., Farlow, M., Iwatsubo, T., Vellas, B., Joffe, S., Kieburtz, K., Raman, R., Sun, X., Aisen, P.S., Siemers, E., Liu-Seifert, H., Mohs, R., Alzheimer's Disease Cooperative Study Steering Committee; Solanezumab Study Group,

2014. Phase 3 trials of solanezumab for mild-to-moderate Alzheimer's disease. N. Engl. J. Med 370, 311–321.
Drzezga, A., Lautenschlager, N., Siebner, H., Riemenschneider, M., Willoch, F., Minoshima, S., Schwaiger, M., Kurz, A., 2003. Cerebral metabolic changes accompanying conversion of mild cognitive impairment into Alzheimer's disease: a PET follow-up study. Eur. J. Nucl. Med. Mol. Imaging 30, 1104–1113.
Games, D., Adam, D., Alessandrini, R., Barbour, R., Berthelette, P., Blakwell, C., Carr, T., Clemens, J., Donaldson, T., Gillespie, F., 1995. Alzheimer-type neuropathology in transgenic mice overexpressing V717F beta-amyloid precursor protein. Nature 373, 523–527.
Glaser, L., Brown, D.H., 1957. The synthesis of chitin in cell-free extracts of Neurospora crassa. J. Biol. Chem 228, 729–742.
Haass, C., Selkoe, D.J., 2007. Soluble protein oligomers in neurodegeneration: lessons from the Alzheimer's amyloid beta-peptide. Nat. Rev. Mol. Cell Biol 8, 101–112.
Holmes, C., Boche, D., Wilkinson, D., Yadegarfar, G., Hopkins, V., Bayer, A., Jones, R.W., Bullock, R., Love, S., Neal, J.W., Zotova, E., Nicoll, J.A., 2008. Long-term effects of Ab42 immunisation in Alzheimer's disease: follow-up of a randomised, placebo controlled phase I trial. Lancet 372, 216–223.
Hsiao, K., Chapman, P., Nilsen, S., Eckman, C., Harigaya, Y., Younkin, S., Yang, F., Cole, G., 1996. Correlative memory deficits, A beta elevation, and amyloid plaques in transgenic mice. Science 274, 99–102.
Ishii, K., Kitagaki, M., Kono, M., Mori, E., 1996. Decreased medial temporal oxygen metabolism in Alzheimer's disease shown by PET. J. Nucl. Med 37, 1159–1165.
Ishii, K., Inamura, T., Sasaki, M., Yamaji, S., Sakamoto, S., Kitagaki, H., Hashimoto, M., Hirono, N., Shimomura, T., Mori, E., 1998. Regional cerebral glucose metabolism in dementia with Lewy bodies and Alzheimer's disease. Neurology 51, 125–130.
Ittner, L.M., Ke, Y.D., Delerue, F., Bi, M., Gladbach, A., van Eersel, J., Wölfing, H., Chieng, B.C., Christie, M.J., Napier, I.A., Eckert, A., Staufenbiel, M., Hardeman, E., Götz, J., 2010. Dendritic function of tau mediates amyloid toxicity in Alzheimer's disease mouse models. Cell 142, 387–397.
Koffie, M.R., Hyman, B.T., Spires-Jones, T.L., 2011. Alzheimer's disease: synapses gone cold. Mol. Neurodegener 6, 63.
Lambert, M.P., Barlow, A.K., Chromy, B.A., Edwards, C., Freed, R., Liosatos, M., Morgan, T.E., Rozovsky, I., Trommer, B., Viola, K.L., Wals, P., Zhang, C., Finch, C.E., Krafft, G.A., Klein, W.L., 1998. Diffusible, nonfibrillar ligands derived from Aβ1-42 are potent central nervous system neurotoxins. Proc. Natl. Acad. Sci. U.S.A 95, 6448–6453.
Lee, C.G., Da Silva, C.A., Lee, J.Y., Hartl, D., Elias, J.A., 2008. Chitin regulation of immune responses: an old molecule with new roles. Curr. Opin. Immunol 20, 684–689.
Lemere, C.A., Masliah, E., 2010. Can Alzheimer disease be prevented by amyloid-beta immunotherapy? Nat. Rev. Neurol 6, 108–119.
Lewis, J., Dickson, D.W., Lin, W.L., Chisholm, L., Corral, A., Jones, G., Yen, S.H., Sahara, N., Skipper, L., Yager, D., Eckman, C., Hardy, J., Hutton, M., McGowan, E., 2001. Enhanced neurofibrillary degeneration in transgenic mice expressing mutant tau and APP. Science 293, 1487–1491.
Li, S., Hong, S., Shepardson, N.E., Walsh, D.M., Shankar, G.M., Selkoe, D., 2009. Soluble oligomers of amyloid β protein facilitate hippocampal long-term depression by disrupting neuronal glutamate uptake. Neuron 62, 788–801.
Li, S., Jin, M., Koeglsperger, T., Shepardson, N.E., Shankar, G.M., Selkoe, D.J., 2011. Soluble Ab oligomers inhibit long-term potentiation through a mechanism involving excessive activation of extrasynaptic NR2B-containing NMDA receptors. J. Neurosci 31, 6627–6638.
Love, D.C., Hanover, J.A., 2005. The hexosamine signaling pathway: deciphering the O-GlcNAc code. Sci. STKE 13, 654–662.
Meda, L., Cassatella, M.A., Szendrei, G.I., Otvos Jr., L., Baron, P., Villalba, M., Ferrari, D., Rossi, F., 1995. Activation of microglial cells by beta-amyloid protein and interferon-gamma. Nature 374, 647–650.
Minoshima, S., Frey, K.A., Koeppe, R.A., Foster, N.L., Kuhl, D.E., 1995. A diagnostic approach in Alzheimer's disease using three-dimensional stereotactic surface projections of fluorine-18-FDG PET. J. Nucl. Med 36, 1238–1248.
Muzzarelli, R.A., 1997. Human enzymatic activities related to the therapeutic administration of chitin derivatives. Cell Mol. Life Sci 53, 131–140.
Nishimura, K., Nishimura, S., Nishi, N., Saiki, I., Tokura, S., Azuma, I., 1984. Immunological activity of chitin and its derivatives. Vaccine 2, 93–99.
Nomura, I., Kato, N., Kita, T., Takechi, H., 2005. Mechanism of impairment of long-term potentiation by amyloid beta is independent of NMDA receptors or voltage-dependent calcium channels in hippocampal CA1 pyramidal neurons. Neurosci. Lett 391, 1–6.
Nowotny, P., Hinrichs, A.L., Smemo, S., Kauwe, J.S., Maxwell, T., Holmans, P., Hamshere, M., Turic, D., Jehu, L., Hollingworth, P., Moore, P., Bryden, L., Myers, A., Doil, L.M., Tacey, K.M., Gibson, A.M., McKeith, I.G., Perry, R.H., Morris, C.M., Thal, L., Morris, J.C., O'Donovan, M.C., Lovestone, S., Grupe, A., Hardy, J., Owen, M.J., Williams, J., Goate, A., 2005. Association studies between risk for late-onset Alzheimer's disease and variants in insulin degrading enzyme. Am. J. Med. Genet. B Neuropsychiatr. Genet 136, 62–68.
Oakley, H., Cole, S.L., Logan, S., Maus, E., Shao, P., Craft, J., Guillozet-Bongaarts, A., Ohno, M., Disterhoft, J., Van Eldik, L., Berry, R., Vassar, R., 2006. Intraneuronal beta-amyloid aggregates, neurodegeneration, and neuron loss in transgenic mice with five familial Alzheimer's disease mutations: potential factors in amyloid plaque formation. J. Neurosci 26, 10129–10140.
O'Callaghan, P., Sandwall, E., Li, J.P., Yu, H., Ravid, R., Guan, Z.Z., van Kuppevelt, T.H., Nilsson, L.N., Ingelsson, M., Hyman, B.T., Kalimo, H., Lindahl, U., Lannfelt, L., Zhang, X., 2008. Heparan sulfate accumulation with Abeta deposits in Alzheimer's disease and Tg2576 mice is contributed by glial cells. Brain Pathol 18, 548–561.
Oddo, S., Caccamo, A., Kitazawa, M., Tseng, B.P., La Ferla, F.M., 2003. Amyloid deposition precedes tangle formation in a triple transgenic model of Alzheimer's disease. Neurobiol. Aging 24, 1063–1070.
Piert, M., Koeppe, R.A., Giordani, B., Berent, S., Kuhl, D.E., 1996. Diminished glucose transport and phosphorylation in Alzheimer's disease determined by dynamic FDG-PET. J. Nucl. Med 37, 201–208.
Piras, I., Melis, A., Ghiani, M.E., Falchi, A., Luiselli, D., Moral, P., Varesi, L., Calò, C.M., Vona, G., 2007. Human CHIT1 gene distribution: new data from Mediterranean and European populations. J. Hum. Genet 52, 110–116.
Querfurth, H.W., La Ferla, F.M., 2010. Alzheimer's Disease. N. Engl. J. Med 362, 329–344.
Raymond, C.R., Ireland, D.R., Abraham, W.C., 2003. NMDA receptor regulation by amyloid-β does not account for its inhibition of LTP in rat hippocampus. Brain Res 968, 263–272.
Salloway, S., Sperilng, R., Fox, N.C., Blennow, K., Klunk, W., Raskind, M., Sabbagh, M., Honig, L.S., Porsteinsson, A.P., Ferris, S., Reichert, M., Ketter, N., Nejadnik, B., Guenzler, V., Miloslavsky, M., Wang, D., Lu, Y., Lull, J., Tudor, I.C., Liu, E., Grundman, M., Yuen, E., Black, R., Brashear, H.R., Bapineuzumab 301 and 302 Clinical Trial Investigators, 2014. Two phase 3 trials of bapineuzumab in mild-to-moderate Alzheimer's disease. N. Engl. J. Med 370, 322–333.
Selkoe, D.J., 2008. Soluble oligomers of the amyloid beta-protein impair synaptic plasticity and behaviour. Behav. Brain Res 192, 106–113.
Semino, C.E., Specht, C.A., Raimondi, A., Robbins, P.W., 1996. Homologs of the Xenopus developmental gene DG42 are present in zebrafish and mouse and are involved in the synthesis of Nod-like chitin oligosaccharides during early embryogenesis. Proc. Natl. Acad. Sci. U.S.A 93, 4548–4553.
Shah, K., DeSilva, S., Abbruscato, T., 2012. The Role of Glucose Transporters in Brain Disease: Diabetes and Alzheimer's Disease. Int. J. Mol. Sci 13, 12629–12655.
Shankar, G.M., Bloodgood, B.L., Townsend, M., Walsh, D.M., Selkoe, D.J., Sabatini, B.L., 2007. Natural oligomers of the Alzeimer amyloid-β protein induce reversible synapse loss by modulating an NMDA-type glutamate receptor-dependent signaling pathway. J. Neurosci 27, 2866–2875.
Shankar, G.M., Metha, T.H., Garcia-Munoz, A., Shepardson, N.E., Smith, I., Brett, F.M., Farrell, M.A., Rowan, M.J., Lemere, C.A., Regan, C.M., Walsh, D.M., Sabatini, B.L., Selkoe, D.J., 2008. Amyloid-beta protein dimers isolated directly from Alzheimer's brains impair synaptic plasticity and memory. Nat. Med 14, 837–842.
Shibata, Y., Metzger, W.J., Myrvik, Q.N., 1997. Chitin particle-induced cell-mediated immunity is inhibited by soluble mannan: mannose receptor-mediated phagocytosis initiates IL-12 production. J. Immunol 159, 2462–2467.
Simpson, I.A., Chundu, K.R., Davies-Hill, T., Honer, W.G., Davies, P., 1994. Decreased concentration of GLUT1 and GLUT3 glucose transporters in the brains of patients with Alzheimer's disease. Ann. Neurol 35, 546–551.
Simpson, I.A., Davies, P., 1994. Reduced glucose transporter concentrations in brains of patients with Alzheimer's disease. Ann. Neurol 36, 800–801.
Snyder, E.M., Nong, Y., Almeida, C.G., Paul, S., Moran, T., Choi, E.Y., Nairn, A.C., Salter, M.W., Lombroso, P.J., Gouras, G.K., Greengard, P., 2005. Regulation of NMDA receptor trafficking by amyloid-β. Nature Neurosci 8, 1051–1058.
Sotgiu, S., Piras, M.R., Barone, R., Arru, G., Fois, M.L., Rosati, G., Musumeci, S., 2007. Chitotriosidase and Alzheimer's disease. Curr. Alzheimer Res 4, 295–296.
Sotgiu, S., Musumeci, S., Marconi, S., Gini, B., Bonetti, B., 2008. Different content of chitin-like polysaccharides in multiple sclerosis and Alzheimer's disease brains. J. Neuroimmunol 197, 70–73.
Stine Jr., W.B., Dahlgren, K.N., Krafft, G.A., LaDu, M.J., 2003. In vitro characterization of conditions for amyloid-beta peptide oligomerization and fibrillogenesis. J. Biol. Chem 278, 11612–11622.
Timmer, N.M., Kuiperij, H.B., de Waal, R.M.W., Verbeek, M.M., 2010. Do amyloid β-associated factors co-deposit with Aβ in mouse models for Alzheimer's disease? J. Alzheimer Dis 22, 345–355.
Townsend, M., Shankar, G.M., Mehta, T., Walsh, D.M., Selkoe, D.J., 2006. Effects of secreted oligomers of amyloid beta-protein on hippocampal synaptic plasticity: a potent role for trimers. J. Physiol 572, 477–492.
Turner, P.R., O'Connor, K., Tate, W.P., Abraham, W.C., 2003. Roles of amyloid precursor protein and its fragments in regulating neural activity, plasticity and memory. Prog. Neurobiol 70, 1–32.
Van Horssen, J., Wesseling, P., Van den Heuvel, L.P., de Waal, R.M., Verbeek, M.M., 2003. Heparan sulphate proteoglycans in Alzheimer's disease and amyloid-related disorders. Lancet Neurol 2, 482–492.
Yoshida, M., Itano, N., Yamada, Y., Kimata, K., 2002. In vitro synthesis of hyaluronan by a single protein derived from mouse HAS1 gene and characterization of amino acid residues essential for the activity. J. Biol. Chem 275, 497–506.